Journal of Chemical Health Risks

www.jchr.org

JCHR (2025) 15(6), 571-584 | ISSN:2251-6727

Ibudilast-Loaded Ethosomal Nanogel for Transdermal Management of Osteoarthritis: Formulation, Characterization, and Preclinical Evaluation

[1]Suraj Vishwas, [2]Dr Swarnali Das Paul, [3]Dr Anil Kumar Sahu

[1]Faculty of Pharmaceutical Sciences, Shri Shankaracharya Technical Campus, Bhilai (C.G.)

[2]Shri Shankaracharya College of Pharmaceutical Sciences, SSPU, Bhilai, 490020, C.G., India

[3]Royal College of Pharmacy, Raipur (C.G.)

*Corresponding author:

Suraj Vishwas, Faculty of Pharmaceutical Sciences, Shri Shankaracharya Technical Campus, Bhilai (C.G.)

(Received: 27 September 2025 Revised: 05 October 2025 Accepted: 10 November 2025)

KEYWORDS

Ibudilast, nanogel, osteoarthritis, PDE inhibitor, transderma delivery, monosodium iodioacetate.

ABSTRACT:

Osteoarthritis (OA), a common degenerative joint disease characterized by cartilage degradation and inflammation, can be effectively managed with phosphodiesterase (PDE) inhibitors, which provide both anti-inflammatory and chondroprotective benefits. In the present study, ibudilast-loaded ethosomes were formulated using the cold method and subsequently incorporated into a gel based on Carbopol 934 to develop a transdermal nanogel delivery system. The developed ethosome exhibited a mean hydrodynamic diameter of 193.20 ± 0.85 nm with a narrow size distribution (PDI: 0.264 ± 0.002), a negative surface charge indicated by a zeta potential of -28.3 ± 0.32 mV, and an entrapment efficiency of 79.83 ± 0.22%. The nanogel demonstrated suitable pH, viscosity, spreadability, and sustained in vitro release of ibudilast. The topical PDE inhibitor nanogel demonstrated superior therapeutic efficacy compared to the plain ibudilast gel in MIA-induced OA rats, providing strong reassurance of its potential. The Treatment group exhibited a significant reduction in oxidative stress markers (MDA: 5.56 ± 1.05 µmol/L), a reassuring sign of the treatment's effectiveness. Restoration of antioxidant levels (CAT: 49.33 ± 4.05 U/mg, SOD: 20.76 ± 1.99 U/mg, GSH: 40.11 ± 2.73 µmol/mg) and normalization of inflammatory cytokines (TNF-α: 36.16 ± 3.06 pg/mL, IL-1β: 16.65 ± 1.41 pg/mL, IL-10: 27.66 ± 4.58 pg/mL). Histopathological analysis confirmed reduced cartilage erosion, minimal synovial hyperplasia, and improved chondrocyte architecture in the treated group. In conclusion, the study demonstrates that the Ibudilast-loaded nanogel holds significant potential as an effective transdermal therapeutic strategy for managing osteoarthritis.

1. Introduction

Osteoarthritis (OA) is a common degenerative joint disorder characterized by persistent inflammation, cartilage breakdown, and ongoing pain [1]. A key feature of OA is the heightened expression of pro-inflammatory cytokines, such as interleukin-1 beta (IL-1β), tumor necrosis factor-alpha (TNF-α), and interleukin-6 (IL-6), which contribute significantly to joint deterioration [2]. Additionally, patients with OA often show reduced activity of antioxidant enzymes, including glutathione (GSH), catalase (CAT), and superoxide dismutase (SOD), resulting in elevated oxidative stress that further promotes cartilage damage and inflammation [3].

Phosphodiesterase (PDE) inhibitors are medications that prevent the breakdown of cyclic nucleotides, specifically cyclic adenosine monophosphate (cAMP) and cyclic guanosine monophosphate (cGMP), by blocking PDE enzymes. This inhibition elevates intracellular levels of cAMP or cGMP, influencing a range of cellular processes, including inflammation, immune responses, and smooth muscle relaxation [4]. PDE inhibitors are classified according to the specific PDE isoenzyme they target, such as PDE1, PDE2, PDE3, PDE4, and PDE5, each of which regulates

Journal of Chemical Health Risks

www.jchr.org

JCHR (2025) 15(6), 571-584 | ISSN:2251-6727

distinct cellular functions. Among these, PDE4 inhibitors have shown particular potential in controlling inflammatory conditions by suppressing pro-inflammatory cytokines [5]. Consequently, PDE4-targeted inhibitors have emerged as promising agents for modulating the inflammatory pathways implicated in osteoarthritis.

Ibudilast, a pyrazolo-pyridine derivative, acts as a broad-spectrum phosphodiesterase (PDE) inhibitor, targeting PDEs 3, 4, 10, 11, and 12. By increasing intracellular cyclic adenosine monophosphate (cAMP) levels, ibudilast helps suppress the production of pro-inflammatory cytokines, thereby reducing inflammation and protecting against cartilage degradation. Moreover, ibudilast has been reported to facilitate the clearance of pathogenic protein aggregates, indicating potential benefits in alleviating oxidative stress-related tissue damage [6].

The present study aimed to investigate the therapeutic potential of a phosphodiesterase (PDE) inhibitor in an osteoarthritis model, explicitly focusing on Ibudilast, whose efficacy in osteoarthritis has not been previously examined. Considering the inflammatory and degenerative mechanisms underlying osteoarthritis, along with Ibudilast's known anti-inflammatory and neuroprotective effects [7], it was hypothesized that the drug could exert disease-modifying benefits. However, due to its poor oral bioavailability and limited systemic targeting, a transdermal delivery approach was deemed the optimal choice. To enable effective and localized drug delivery to the affected joint, a nanogel-based formulation was developed. Polymeric nanogels have emerged as advanced carriers for transdermal therapy, offering enhanced skin penetration, protection of the drug from degradation, and controlled, sustained release [8]. Additionally, nanogels improve patient compliance through ease of application and the avoidance of hepatic first-pass metabolism [9]. Thus, employing a nanogel system not only addresses the pharmacokinetic limitations of Ibudilast but also facilitates targeted delivery, potentially enhancing therapeutic outcomes in osteoarthritis management.

The cold method is a straightforward, efficient, and widely adopted technique for preparing ethosomes. In this approach, phospholipids are dissolved in ethanol under constant stirring, followed by the addition of the drug to ensure uniform solubilization. Water is then gradually incorporated at room temperature with continuous mixing, resulting in the spontaneous formation of ethosomal vesicles. Ethanol contributes to vesicle flexibility, enhances drug solubility, and promotes skin permeation. The resulting formulation is stored at low temperatures to maintain stability. This method is favored as it yields stable, nanosized vesicles with high drug entrapment efficiency and superior penetration properties. For the development of the transdermal nanogel, Carbopol 934 was selected due to its high viscosity, mucoadhesive characteristics, and ability to form stable hydrogels suitable for dermal application [10]. Triethanolamine was employed to neutralize the acidic Carbopol dispersion, facilitating gel formation and adjusting the pH to a skin-compatible range (6.0–6.5). Together, these components enabled the creation of a stable nanogel system designed to improve the transdermal delivery of Ibudilast for osteoarthritis therapy.

2. Experimental methods

2.1 Chemicals and Reagents

Ibudilast, soya lecithin, and monosodium iodoacetate were procured from Otto Chemie Pvt Ltd. All other chemicals used in the study were of analytical grade.

2.2 Preparation of ethosomal suspension

Ethosomes were formulated following the method described by Touitou et al. (2000) [11] with slight modifications. Briefly, lecithin (4% w/v) was dissolved in ethanol (30% v/v) containing ibudilast (1%) using a magnetic stirrer in a round-bottom flask, which was kept covered to minimize ethanol loss. Thereafter, distilled water was gradually added under continuous stirring, resulting in the formation of ethosomal colloidal dispersions. The resulting suspension was maintained at room temperature for 30 minutes with constant agitation, after which it was stored under refrigeration until further characterization. The prepared formulations were evaluated for vesicle size, zeta potential, polydispersibility index, morphology, entrapment efficiency, and in vitro drug release behavior.

Journal of Chemical Health Risks

www.jchr.org

JCHR (2025) 15(6), 571-584 | ISSN:2251-6727

2.2.1 Determination of Vesicle Size, Size Distribution, and Zeta Potential

The average vesicle size (VS), polydispersity index (PDI), and zeta potential (ZP) of ibudilast-loaded ethosomes were determined at room temperature using dynamic light scattering (DLS, Anton Paar Litesizer 500). For analysis, the samples were diluted to 0.5% (w/v) with deionized water and subjected to agitation for 3 minutes. This procedure was carried out in triplicate to ensure reproducibility [12].

2.2.2 Field emission scanning electron microscope (FESEM) analysis

The morphological features of ethosomes and nanogels were examined using a field-emission scanning electron microscope (FESEM, Carl Zeiss Ultra-High-Resolution Gemini SEM 500, KMAT, India). A drop of the sample was carefully placed on a clean glass stub, air-dried, and subsequently coated with a thin layer of gold to enhance conductivity. The specimens were then visualized under FESEM at a suitable magnification.

2.2.3 Entrapment efficiency

The entrapment efficiency (%EE) of the prepared ethosomes was determined by calculating the difference between the total drug added and the unentrapped drug. Unencapsulated ibudilast was quantified using a centrifugation method. Briefly, the formulations were centrifuged in an ultracentrifuge (Remi) with a TLA-45 rotor at 14,000 rpm and 4 °C for 30 minutes. The supernatant was carefully collected, and the residue was re-centrifuged for an additional 15 minutes under the same conditions. The total amount of unentrapped drug was then measured using a UV/Vis spectrophotometer at a wavelength of 227 nm. All measurements were performed in triplicate [13]. The percentage of encapsulated drug amount was calculated using the following formula:

%EE = (Amount of the drug in the ethosome /Total amount of drug loaded into the ethosome) ×100

2.2.4 In vitro permeation study

The in vitro drug release of ethosomes and ethosomal nanogel was evaluated using the dialysis bag diffusion method (molecular weight cut-off 12,000 Da). Briefly, 1 mL of each formulation was placed in separate dialysis bags, which were then immersed in 20 mL of PBS buffer and maintained at 37 °C with continuous stirring at 100 rpm. Samples of the release medium were withdrawn at predetermined intervals (0.5, 1, 2, 4, 6, 8, 12, 16, 20, and 24 hours) and replaced with an equal volume of fresh buffer. The amount of ibudilast released was quantified using UV–visible spectroscopy [14].

2.3 Formulation of ethosomal nanogel and plain ibudilast gel

The ibudilast-loaded nanogel was prepared by incorporating Carbopol 934 into ibudilast-loaded ethosomes. Briefly, Carbopol 934 (0.75% w/v) was dispersed in distilled water and allowed to hydrate for 1 hour. The pH of the dispersion was then adjusted to 6–6.5 using triethanolamine. Ibudilast-loaded ethosomes were added to the hydrated Carbopol dispersion and gently stirred at 1200 rpm for 15 minutes (Remi Motors Ltd., India) to obtain the ethosomal nanogel. For comparison, a plain ibudilast gel was prepared by dissolving the drug in methanol and mixing it with Carbopol 934 (0.75% w/v) under the same stirring conditions for 15 minutes to achieve a uniform gel. The final concentration of ibudilast in both the ethosomal nanogel and the plain gel was 3% [15].

2.4 Characterization of Nanogel

2.4.1 Organoleptic properties

The organoleptic characteristics of the Ibudilast nanogel, including color, uniformity, and the presence of grittiness, were evaluated through visual inspection.

2.4.2 Clarity and Refractive Index Determination

The transparency of the formulated Carbopol-based nanogel was examined visually under natural light against both black and white backgrounds to detect any turbidity or suspended particles. For quantitative evaluation, the refractive index was measured using an Abbe-type digital refractometer (Anton Paar) maintained at 25 ± 0.5 °C. A small amount of the nanogel was applied to the prism surface, and readings were recorded once the sample reached equilibrium. Distilled water (n = 1.333 at 25 °C) served as the reference standard to validate the method. All measurements were performed in triplicate, and results were reported as mean ± SD [16].

Journal of Chemical Health Risks

www.jchr.org

JCHR (2025) 15(6), 571-584 | ISSN:2251-6727

2.4.3 Determination of pH

The pH of the Ibudilast nanogel was determined using a digital pH meter (Labcare pH Meter). The instrument was calibrated beforehand with standard buffer solutions of pH 4 and 7. For analysis, about 1 g of the nanogel was dispersed in 100 mL of distilled water, and the pH value was measured in triplicate (n = 3) [17].

2.4.4 Viscosity measurement

The rheological behavior of the Ibudilast-loaded nanogel was evaluated using a programmable Brookfield viscometer (Model DV2T Plus, AMETEK Brookfield, Middleboro, MA, USA) at 25 °C with Spindle LV-4. The spindle was carefully immersed vertically into the gel without touching the container walls. Measurements were taken at rotational speeds ranging from 2 to 50 rpm, with readings recorded after 1 minute once the gel level had stabilized. Prior to each test, the sample was equilibrated at 25 °C. The results were expressed as viscosity versus shear rate plots [18].

2.4.5 Percent (%) drug content

The content uniformity of the Ibudilast nanogel was evaluated by diluting 0.5 mL of the formulation with double-distilled water, followed by dissolution in 5 mL of ethanol using vortex mixing. The resulting solution was filtered through a 0.45 µm membrane filter, and the drug concentration in the filtrate was analyzed using UV–Visible spectrophotometry (UV-1700, Shimadzu, Japan) at 227 nm to ensure accuracy and reliability of the results.

$$(\%)\ \text{Content of Ibudilast} = \frac{amount\ of\ drug\ detected}{amount\ of\ drug\ employed} \times 100$$

2.4.6 Spreadability

The spreadability of the Ibudilast-nanogel was evaluated by placing 0.5 g of the formulation within a 1 cm diameter circle on a glass plate. A second glass plate weighing 250 g was then placed on top and left for 1 minute. The increase in diameter resulting from the gel's spreading provided a measure of its spreadability, an important parameter for its practical application in pharmaceutical and nanotechnological formulations.

2.4.7 Experimental Animals

Male Albino Wistar rats weighing 180–200 g were employed in the study and housed individually under controlled conditions, with a temperature of 25 ± 1 °C and relative humidity of 45–60%. The animals had free access to food and water and were acclimatized for 10 days prior to the experiment. The experimental protocol was approved by the Committee for Control and Supervision of Experiments on Animals (CCSEA), Government of India (Registration No. RIPS/IAEC/2023-24/08/08) [19].

2.4.8 Analgesic activity (Hot-plate method)

The analgesic activity of the prepared Ibudilast nanogel was assessed using the hot-plate method. Albino Sprague-Dawley rats weighing 180–200 g were randomly assigned to three groups (n = 6 per group). The control group received a topical vehicle, while Treatment Group 1 (T1) and Treatment Group 2 (T2) were administered topically with plain Ibudilast gel (equivalent to 10 mg of ibudilast) and Ibudilast-loaded nanogel (equivalent to 10 mg of ibudilast), respectively. Animals were placed on a heated plate (Eddy's hot plate) maintained at 50-55 °C, and the reaction time (latency) to thermal stimuli, indicated by paw licking or jumping, was recorded. Baseline latency was measured prior to topical application, and subsequent measurements were taken 30 minutes after treatment to evaluate the analgesic effect of the formulations.

2.4.9 Experimental Design for anti-osteoarthritic activity

An osteoarthritis model in albino rats was established using monosodium iodoacetate (MIA). Twenty-four rats were randomly divided into four groups of six animals each. The normal group received a single intra-articular injection of normal saline (50 µL), while osteoarthritis was induced in the OA-control, Treatment Group 1 (T1), and Treatment Group 2 (T2) groups via a single intra-articular injection of MIA (3 mg in 50 µL). Treatments commenced one day after MIA administration and continued for 21 days. The normal and OA-control groups received a placebo, whereas T1 was treated with topical plain Ibudilast gel (10 mg equivalent of ibudilast) applied twice daily to the left knee joint. T2 received topical Ibudilast ethosome-loaded Carbopol nanogel (10 mg equivalent of

Journal of Chemical Health Risks

www.jchr.org

JCHR (2025) 15(6), 571-584 | ISSN:2251-6727

ibudilast) applied twice daily to the left knee joint. Treatment efficacy was evaluated by monitoring body weight and paw volume on days 7, 14, and 21 using a digital balance and a calibrated digital caliper [20].

2.4.10 Blood Collection and Determination of Hematological Parameters

The animals were fasted overnight and anesthetized with an overdose of ketamine and xylazine. Blood samples were collected via cardiac puncture and divided into two portions for analysis. The first portion was used to assess hematological parameters, including red blood cell (RBC) count, white blood cell (WBC) count, and haemoglobin (Hb) levels. The second portion was analyzed for arthritis-related inflammatory markers, such as tumor necrosis factor-alpha (TNF-α), interleukin-beta (IL-β), and IL-10, as well as oxidative stress indicators, including catalase (CAT), superoxide dismutase (SOD), glutathione (GSH), and malondialdehyde (MDA). Serum separation was achieved by centrifuging the blood at 10,000 rpm for 10 minutes [21].

Hematological parameters were determined using a haematology analyzer or manually with a hemacytometer after appropriate staining, while Hb levels were measured using the cyanmethemoglobin method or an automated analyzer with spectrophotometric detection. Inflammatory cytokines (TNF-α, IL-β, and IL-10) were quantified using an enzyme-linked immunosorbent assay (ELISA) on centrifuged serum, and concentrations were determined using a microplate reader.

Oxidative stress markers were evaluated as follows, CAT activity was measured based on hydrogen peroxide decomposition at 240 nm, SOD activity was determined by its ability to inhibit nitroblue tetrazolium (NBT) reduction at 560 nm, GSH levels were quantified using Ellman's reagent (DTNB), forming a yellow complex read at 412 nm, and MDA levels were assessed using the thiobarbituric acid reactive substances (TBARS) assay, where MDA reacts with TBA to produce a colored complex measured at 532 nm. These analyses provided detailed insights into the inflammatory response and oxidative stress under the experimental conditions.

2.4.11 Tissue Preparation for Histopathology

After macroscopic examination, samples of the knee joint were collected for histological evaluation. The specimens were fixed in 10% formaldehyde prepared in 0.1 M phosphate-buffered saline (pH 7.4) and preserved for approximately three days. Decalcification was performed using 5% formic acid for 11–12 days, with older animals requiring longer durations. Following decalcification, the samples were embedded in paraffin and sectioned frontally through the femorotibial joint. Histopathological analysis was conducted using a light microscope, with tissue sections stained with hematoxylin and eosin (H&E). All assessments were performed in a blinded manner to ensure unbiased interpretation [22].

2.4.12 Statistical analysis

GraphPad Prism software (version 5.0, GraphPad Software, Inc., USA) was used for data analysis. Pharmacological study results were expressed as mean ± standard deviation (SD). Statistical significance among multiple groups was assessed using two-way ANOVA, followed by Bonferroni's and Tukey's post hoc tests for pairwise comparisons.

3. Results and Discussion

3.1 Characterization of ethosomes

The average vesicle size (VS) of the formulation was 193.20 ± 0.85 nm (Figure 1A), with polydispersity index (PDI) values below 0.264 ± 0.002, confirming a narrow and homogeneous particle size distribution. The zeta potential (ZP) was recorded as -28.3 ± 0.32 mV (Figure 1B), indicating a highly negative surface charge attributed to the presence of ethanol, which enhances the stability of ethosomes and minimizes the risk of flocculation. The prepared ethosomes were evaluated for their physicochemical characteristics. Scanning electron microscopy (SEM) revealed that the vesicles were predominantly spherical in shape with smooth surfaces, uniform morphology, and discrete distribution without notable aggregation, suggesting good dispersibility (Figure 1C). Furthermore, the formulation exhibited a high entrapment efficiency of 79.83 ± 0.22%, consistent with reported findings, thereby validating the method employed for achieving efficient drug loading.

Journal of Chemical Health Risks

www.jchr.org

JCHR (2025) 15(6), 571-584 | ISSN:2251-6727

3.2 Characterization of nanogel

The PDE4 inhibitor-loaded ethosomal nanogel formulation was thoroughly evaluated for its physical characteristics, drug content, and performance to ensure suitability for transdermal delivery. The formulation appeared transparent, aesthetically appealing, and easy to apply. SEM analysis of the Carbopol nanogel (Figure 1D) revealed a fibrous, interconnected, and porous network typical of hydrated polymeric gels, along with a smooth surface free from cracks or phase separation, confirming its stability and uniformity. The nanogel displayed excellent clarity with a refractive index of 1.337 ± 0.002, indicating the absence of suspended particles, while the ibudilast-loaded Carbopol 934 nanogel exhibited good homogeneity with no clogs. The pH was recorded at 6 ± 0.5, within the physiological range, indicating compatibility with the skin and a minimal risk of irritation. Spreadability was favorable, with a diameter of 6.2 ± 1 cm, supporting even application and improved absorption. Rheological evaluation revealed pseudoplastic flow behavior, characterized by a decrease in viscosity as the shear rate increased (2–50 rpm), thereby enhancing the ease of spreading (Figure 2A). The drug content was found to be 97.95 ± 0.5%, reflecting efficient drug incorporation. In vitro release studies using dialysis membrane diffusion in phosphate-buffered saline (pH 7.4, 37 ± 0.5°C) demonstrated rapid release from ibudilast-loaded ethosomes, with 78.4% released within 8 hours, whereas the ethosomal nanogel exhibited a controlled and sustained release profile, achieving 86.7% cumulative release over 24 hours, highlighting the gel matrix's role in prolonging drug diffusion and ensuring sustained therapeutic action (Figure 2B).

3.3 In-Vivo Animal Study

3.3.1 Analgesic activity

Figure 3A illustrates the analgesic effect of the formulations. Both the T1 and T2 treatment groups showed a significant increase in latency time compared to the control group, indicating the enhanced analgesic potential of the Ibudilast nanogel.

3.3.2 Body weight

The average body weight of rats in all experimental groups was measured before and after treatment, as shown in Figure 3B. Following the induction of osteoarthritis, all groups experienced a reduction in body weight. After the onset of treatment, the treated groups exhibited weight gain comparable to that of the normal control group, whereas the arthritic control group continued to show a decrease in body weight.

3.3.3 Paw Volume

Following MIA injection, noticeable symptoms, including knee joint swelling, redness, and restricted movement, appeared from day 1 and peaked by day 4. Treatment with the ethosomal nanogel commenced on day 0 and continued for 21 days. By day 7, rats treated with the nanogel exhibited a significant reduction in joint swelling compared to other MIA-induced groups (Figure 3C). Although no statistically significant differences in swelling were observed among the MIA-injected groups on days 7, 14, and 21, joint swelling gradually decreased across all groups, with the most pronounced improvements seen in rats receiving the Ibudilast nanogel.

3.3.4 Hematological Parameters

Rats treated with plain Ibudilast gel and Ibudilast-loaded nanogel showed a reduction in WBC counts alongside increases in RBC and hemoglobin levels compared to the arthritic control group (Figure 4). These findings indicate notable hematological improvements, including elevated hemoglobin and decreased WBC counts, following treatment.

3.3.5 Serum Biomarkers and Biochemical Parameters

Effect on IL-1β, IL-10 and TNF-α Level

The inflammatory response in MIA-induced osteoarthritis (OA) rats was evaluated by assessing the levels of tumor necrosis factor-alpha (TNF-α), interleukin-1 beta (IL-1β), and interleukin-10 (IL-10). The OA group exhibited a significant increase in pro-inflammatory cytokines, including TNF-α, IL-1β, and IL-10, compared to the normal control group ($p < 0.05$). Specifically, TNF-α levels increased from 24.5 ± 3.27 pg/mL in the normal group to 76.16 ± 5.38 pg/mL in the OA group, while IL-1β levels rose from 8.68 ± 0.87 pg/mL to 45.48 ± 5.76 pg/mL, and IL-10 levels also raised from 22.66 ± 4.63 pg/mL to 65.33 ± 4.45 pg/mL indicating a strong inflammatory response.

Journal of Chemical Health Risks

www.jchr.org

JCHR (2025) 15(6), 571-584 | ISSN:2251-6727

Treatment with plain ibudilast gel (T1) and PDE4 inhibitor-loaded nanogel (T2) significantly ($p < 0.05$) reduced inflammatory cytokine levels while restoring IL-10 levels. The T1 group (plain ibudilast gel) demonstrated a moderate decrease in TNF-α (49.67 ± 7.06 pg/mL) and IL-1β (21.4 ± 3.53 pg/mL), along with a decrease in IL-10 (40.83 ± 4.58 pg/mL), indicating its anti-inflammatory potential. However, the T2 group (PDE4 inhibitor-loaded nanogel) exhibited the most substantial reduction in TNF-α (36.16 ± 3.06 pg/mL), IL-1β (16.65 ± 1.41 pg/mL), and, alongside a significant decrease in IL-10 (27.67 ± 4.58 pg/mL), suggesting superior anti-inflammatory efficacy compared to T1 (Figure 5) [23].

3.3.6 Effect on CAT, SOD, GSH, and MDA

The assessment of serum antioxidant markers, including catalase (CAT), superoxide dismutase (SOD), glutathione (GSH), and malondialdehyde (MDA), provided critical insights into the levels of oxidative stress and the therapeutic effects of ibudilast formulations in osteoarthritis (OA). The MIA-induced osteoarthritis group (OA) exhibited a significant decline ($p < 0.05$) in antioxidant enzyme levels compared to the normal control, confirming oxidative stress-induced damage. Specifically, CAT levels decreased from 58.83 ± 5.21 U/mg in the normal group to 23.16 ± 5.41 U/mg in the OA group, SOD levels dropped from 25.05 ± 2.65 U/mg to 6.55 ± 1.11 U/mg, and GSH levels were reduced from 52.16 ± 4.24 µM to 19.85 ± 2.88 µM, highlighting a severe compromise in antioxidant defense. Additionally, MDA levels, a key indicator of lipid peroxidation, increased from 3.4 ± 0.6 nmol/mg in the normal group to 15.15 ± 1.69 nmol/mg in the OA group, demonstrating heightened oxidative damage.

Following treatment, both the plain ibudilast gel (T1) and PDE4 inhibitor-loaded nanogel (T2) groups exhibited a significant ($p < 0.05$) improvement in antioxidant levels and a reduction in oxidative stress markers. The T1 group showed a partial restoration of CAT (38.66 ± 4.17 U/mg), SOD (13.7 ± 1.40 U/mg), and GSH (30.86 ± 3.25 µM) levels, with MDA levels decreasing to 8.93 ± 0.59 nmol/mg, indicating a moderate protective effect. However, the T2 group (PDE4 inhibitor-loaded nanogel) demonstrated the most substantial recovery, with CAT, SOD, and GSH levels increasing to 49.83 ± 4.05 U/mg, 20.76 ± 1.99 U/mg, and 40.11 ± 2.73 µM, respectively, while MDA levels significantly dropped to 5.56 ± 1.05 nmol/mg (Figure 6). This suggests that the nanogel formulation provided superior oxidative protection, likely due to its enhanced drug retention, sustained release, and improved bioavailability at the affected joint site [24].

3.3.7 Histopathological Examination

Histopathological analysis of femorotibial joint sections revealed marked differences in cartilage integrity among the experimental groups, highlighting the therapeutic effects of Ibudilast formulations (Figure 7). The normal control group (Figure 7A) displayed intact articular cartilage with well-organized chondrocytes, a smooth surface, and no signs of inflammatory infiltration. In contrast, the OA control group (Figure 7B) exhibited severe cartilage degradation, including extensive chondrocyte loss, fibrillation, matrix erosion, and synovial hyperplasia, indicative of advanced osteoarthritis.

Treatment with plain Ibudilast gel (Figure 7C) resulted in moderate improvement, characterized by partial chondrocyte restoration, a roughened yet structurally recovering cartilage surface, and reduced synovial inflammation. However, small areas of fibrosis and residual structural damage persisted, suggesting incomplete regeneration over the 21-day period.

The PDE4 inhibitor-loaded nanogel-treated group (Figure 7D) demonstrated superior cartilage repair, with a smoother articular surface, markedly reduced chondrocyte degeneration, and near-complete restoration of the cartilage matrix. Additionally, this group showed minimal inflammatory cell infiltration, decreased synovial hyperplasia, and negligible fibrosis, underscoring the enhanced therapeutic potential of the nanogel formulation in osteoarthritis management [25].

4. Discussion

The monosodium iodoacetate (MIA) model, which mimics clinical osteoarthritis (OA), was employed to evaluate the effects of ibudilast-loaded nanogels. MIA-induced joint edema peaked between days 4 and 21, with nanogel treatment significantly reducing swelling. Over 21 days, TNF-α and IL-1β levels decreased, with the nanogel-treated groups showing significantly lower cytokine levels, which approached normal by day 21. Two-way ANOVA ($P<0.05$) confirmed the superior

Journal of Chemical Health Risks

www.jchr.org

JCHR (2025) 15(6), 571-584 | ISSN:2251-6727

anti-inflammatory effect of nanogel compared to plain ibudilast gel.

The results from biochemical, hematological, and histopathological evaluations collectively highlight the therapeutic potential of a PDE inhibitor nanogel in the management of osteoarthritis (OA). The OA control group exhibited severe oxidative stress, inflammation, and hematological imbalances, as evidenced by elevated malondialdehyde (MDA) levels (15.15 ± 1.69 µmol/L), increased TNF-α (76.16 ± 5.38 pg/mL). IL-1β (45.48 ± 5.76 pg/mL) and IL-10 levels (65.33 ± 4.45 pg/mL) were significantly depleted, along with significant depletion in antioxidant enzymes (CAT: 23.16 ± 5.41 U/mg, SOD: 6.55 ± 1.11 U/mg, GSH: 19.85 ± 2.88 µmol/mg). Additionally, WBC count was elevated (15.76 ± 1.38 × 10^3 cells/µL), while RBC (5.71 ± 0.97 × 10^6 cells/µL) and hemoglobin (Hb: 6.26 ± 1.14 g/dL) levels were significantly reduced, indicating systemic inflammation and anemia.

Treatment with a PDE inhibitor nanogel (T2) demonstrated superior efficacy compared to plain ibudilast gel (T1), as evidenced by biochemical and histopathological improvements. The T2 group exhibited a significant reduction in oxidative stress markers (MDA: 5.56 ± 1.05 µmol/L), restoration of antioxidant levels (CAT: 49.83 ± 4.05 U/mg, SOD: 20.76 ± 1.99 U/mg, GSH: 40.11 ± 2.73 µmol/mg), and normalization of inflammatory cytokines (TNF-α: 36.16 ± 3.06 pg/mL, IL-1β: 16.65 ± 1.41 pg/mL, IL-10: 27.66 ± 4.58 pg/mL). Hematological parameters also improved significantly (RBC: 7.56 ± 1.11 × 10^6 cells/µL, WBC: 8.13 ± 2.12 × 10^3 cells/µL, Hb: 13.11 ± 1.50 g/dL), suggesting a reduction in systemic inflammation and improved erythropoiesis.

Histopathological assessment of femorotibial joint sections revealed marked differences in cartilage integrity among the study groups, underscoring the therapeutic effects of ibudilast-based formulations. The normal control group exhibited well-preserved articular cartilage, characterized by a uniform arrangement of chondrocytes, a smooth surface morphology, and no evidence of inflammatory infiltration. In contrast, the osteoarthritis (OA) control group exhibited pronounced cartilage destruction, characterized by severe chondrocyte depletion, surface fibrillation, matrix breakdown, and synovial hyperplasia, reflecting advanced disease progression. Treatment with plain ibudilast gel resulted in moderate improvement, as evidenced by partial chondrocyte recovery, a surface showing signs of repair yet still roughened, and a reduction in synovial inflammation. Nonetheless, focal fibrosis and residual structural damage persisted, suggesting that full regeneration was not achieved within the 21-day treatment window. Notably, the PDE4 inhibitor-loaded nanogel group demonstrated the most effective cartilage repair, characterized by a nearly restored matrix, a smoother articular surface, minimal chondrocyte degeneration, and significantly reduced inflammatory infiltration and synovial hyperplasia. Minimal fibrosis was observed, highlighting the nanogel's superior therapeutic efficacy in OA management. These results suggest that PDE inhibitor-loaded nanogels hold promise as an effective transdermal strategy for managing osteoarthritis.

5. Conclusions

The study demonstrates that ibudilast-loaded ethosomal nanogel is a promising formulation for managing MIA-induced osteoarthritis in rats. The characterization of ethosomes revealed a uniform vesicle size, narrow polydispersity, and a highly negative zeta potential, indicating stable and well-dispersed vesicles with high entrapment efficiency. The ethosomal nanogel exhibited favorable physical properties, including transparency, a suitable pH, good spreadability, pseudoplastic rheology, and a high drug content, all of which support its suitability for transdermal application. In vitro release studies confirmed that while ibudilast-loaded ethosomes released the drug rapidly, incorporation into the nanogel provided sustained and controlled release over 24 hours, highlighting the gel matrix's role in prolonging drug diffusion. In vivo, treatment with the nanogel significantly alleviated OA-associated symptoms, including joint swelling and pain, while restoring body weight and improving hematological parameters. Biochemical analysis demonstrated that the nanogel effectively reduced pro-inflammatory cytokines (TNF-α, IL-1β) and regulated IL-10 levels, indicating potent anti-inflammatory activity. Additionally, the formulation enhanced antioxidant defenses, as evidenced by increased CAT, SOD, and GSH levels, and reduced MDA, suggesting a mitigation of oxidative stress. Histopathological evaluation corroborated these findings, showing superior cartilage preservation,

Journal of Chemical Health Risks

www.jchr.org

JCHR (2025) 15(6), 571-584 | ISSN:2251-6727

reduced synovial inflammation, and near-complete restoration of the joint matrix in rats treated with nanogel compared to those treated with plain ibudilast gel and untreated OA controls. Overall, the results indicate that ibudilast-loaded ethosomal nanogel provides enhanced therapeutic efficacy through improved drug delivery, sustained release, anti-inflammatory effects, and oxidative stress mitigation. This formulation presents a promising transdermal strategy for managing osteoarthritis, potentially enhancing clinical outcomes and patient compliance.

CONFLICT OF INTEREST

The author(s) confirm that this article's content has no conflicts of interest.

ACKNOWLEDGEMENTS

Declared none. This project has not received any funding from any sources. The authors thank Rungta College of Pharmaceutical Sciences and Research, Bhilai, for their technical support.

Reference

1. Xia B, Di Chen, Zhang J, Hu S, Jin H, Tong P. Osteoarthritis pathogenesis: a review of molecular mechanisms. Calcif Tissue Int. 2014 Dec;95(6):495-505. doi: 10.1007/s00223-014-9917-9.
2. Nambi G. Does low level laser therapy has effects on inflammatory biomarkers IL-1β, IL-6, TNF-α, and MMP-13 in osteoarthritis of rat models-a systemic review and meta-analysis. Lasers Med Sci. 2021 Apr;36(3):475-484. doi: 10.1007/s10103-020-03124-w.
3. Orhan C, Tuzcu M, Durmus AS, Sahin N, Ozercan IH, Deeh PBD, et al. Protective effect of a novel polyherbal formulation on experimentally induced osteoarthritis in a rat model. Biomed Pharmacother. 2022 Jul;151:113052. doi: 10.1016/j.biopha.2022.113052.
4. Plummer MS, Cornicelli J, Roark H, Skalitzky DJ, Stankovic CJ, Bove S, et al. Discovery of potent, selective, bioavailable phosphodiesterase 2 (PDE2) inhibitors active in an osteoarthritis pain model, part I: transformation of selective pyrazolodiazepinone phosphodiesterase 4 (PDE4) inhibitors into selective PDE2 inhibitors. Bioorg Med Chem Lett. 2013 Jun 1;23(11):3438-42. doi: 10.1016/j.bmcl.2013.03.072.
5. Tenor H, Hedbom E, Häuselmann HJ, Schudt C, Hatzelmann A. Phosphodiesterase isoenzyme families in human osteoarthritis chondrocytes--functional importance of phosphodiesterase 4. Br J Pharmacol. 2002 Feb;135(3):609-18. doi: 10.1038/sj.bjp.0704480.
6. Kishi Y, Ohta S, Kasuya N, Sakita S, Ashikaga T, Isobe M. Ibudilast: a non-selective PDE inhibitor with multiple actions on blood cells and the vascular wall. Cardiovasc Drug Rev. 2001 Fall;19(3):215-25. doi: 10.1111/j.1527-3466.2001.tb00066.x.
7. Clanchy FIL, Williams RO. Ibudilast inhibits chemokine expression in rheumatoid arthritis synovial fibroblasts and exhibits immunomodulatory activity in experimental arthritis. Arthritis Rheumatol. 2019 May;71(5):703-11. doi: 10.1002/art.40787.
8. Tariq L, Arafah A, Ali S, Beigh S, Dar MA, Dar TUH, et al. Nanogel-based transdermal drug delivery system: a therapeutic strategy with under discussed potential. Curr Top Med Chem. 2023;23(1):44-61. doi: 10.2174/1568026622666220818112728.
9. Ahmed S, Alhareth K, Mignet N. Advancement in nanogel formulations provides controlled drug release. Int J Pharm. 2020 Jun 30;584:119435. doi: 10.1016/j.ijpharm.2020.119435.
10. Singh N, Yadav SD, Gupta P, Ali F, Arora S. Dermal delivery of Hypericum perforatum (L.) loaded nanogel: formulation to preclinical psoriasis assessment. Recent Adv Drug Deliv Formul. 2024;18(2):138-54. doi: 10.2174/0126673878288239240415041832.
11. Barupal AK, Gupta V, Ramteke S. Preparation and characterization of ethosomes for topical delivery of aceclofenac. Indian J Pharm Sci. 2010 Sep;72(5):582-6. doi: 10.4103/0250-474X.78519.
12. AlEbadi NN, Al-Lami MS. Formulation and in-vitro evaluation of ethosomes using anastrozole as a modeling drug. Al Mustansiriyah J Pharm Sci. 2022;22(4):90-105.
13. Mishra R, Shende S, Jain PK, Jain V. Formulation and evaluation of gel containing ethosomes

entrapped with tretinoin. J Drug Deliv Ther. 2018 Sep 2;8:315-21.

14. Pathan IB, Jaware BP, Shelke S, Ambekar W. Curcumin loaded ethosomes for transdermal application: formulation, optimization, in-vitro and in-vivo study. J Drug Deliv Sci Technol. 2018 Apr 1;44:49-57.
15. Mujtaba MA, Gangane P, Ali A, Chaudhari S, Kaleem M, More S, et al. Karanjin-loaded soya lecithin-based ethosomal nanogel for the therapeutic intervention of psoriasis: formulation development, factorial design based-optimization, in vitro and in vivo assessment. Biomed Mater. 2024 Jul 11;19(5):055012.
16. Ali A, Ali A, Rahman MA, Warsi MH, Yusuf M, Alam P. Development of nanogel loaded with lidocaine for wound-healing: illustration of improved drug deposition and skin safety analysis. Gels. 2022 Jul 26;8(8):466.
17. Mohammed WH, Ali WK, Al-Awady MJ. Evaluation of in vitro drug release kinetics and antibacterial activity of vancomycin HCl-loaded nanogel for topical application. J Pharm Sci Res. 2018 Nov 1;10(11):2747-56.
18. Pradhan M, Alexander A, Singh M, Singh D, Saraf S, Saraf S, et al. Statistically optimized calcipotriol fused nanostructured lipid carriers for effectual topical treatment of psoriasis. J Drug Deliv Sci Technol. 2020;61:102168. doi: 10.1016/j.jddst.2020.102168.
19. Fareed NY, Kassab HJ. A comparative study of oral diacerein and transdermal diacerein as novasomal gel in a model of MIA induced osteoarthritis in rats. Pharmacia. 2023 Oct 1;70(4).
20. Rao AK, Tiwari R, Gupta N, Rajput D. In vivo evaluation of a novel topical formulation of naproxen and betamethasone nanogel for osteoarthritis. Front Health Inform. 2024 Apr 1;13(3).
21. Chattopadhyay H, Auddy B, Sur T, Gupta M, Datta S. Transdermal co-delivery of glucosamine sulfate and diacerein for the induction of chondroprotection in experimental osteoarthritis. Drug Deliv Transl Res. 2020 Oct;10(5):1327-40.
22. Kawarai Y, Orita S, Nakamura J, Miyamoto S, Suzuki M, Inage K, et al. Changes in proinflammatory cytokines, neuropeptides, and microglia in an animal model of monosodium iodoacetate-induced hip osteoarthritis. J Orthop Res. 2018 Nov;36(11):2978-86.
23. Saleh AS, Abdel-Gabbar M, Gabr H, Shams A, Tamur S, Mahdi EA, Ahmed OM. Ameliorative effects of undifferentiated and differentiated BM-MSCs in MIA-induced osteoarthritic Wistar rats: roles of NF-κB and MMPs signaling pathways. Am J Transl Res. 2024 Jul 15;16(7):2793.
24. Hamdalla HM, Ahmed RR, Galaly SR, Naguib IA, Alghamdi BS, Ahmed OM, et al. Ameliorative effect of curcumin nanoparticles against monosodium iodoacetate-induced knee osteoarthritis in rats. Mediators Inflamm. 2022;2022:8353472.
25. Tsai SW, Lin CC, Lin SC, Wang SP, Yang DH. Isorhamnetin ameliorates inflammatory responses and articular cartilage damage in the rats of monosodium iodoacetate-induced osteoarthritis. Immunopharmacol Immunotoxicol. 2019 Jul 4;41(4):504-12.

Journal of Chemical Health Risks

www.jchr.org

JCHR (2025) 15(6), 571-584 | ISSN:2251-6727

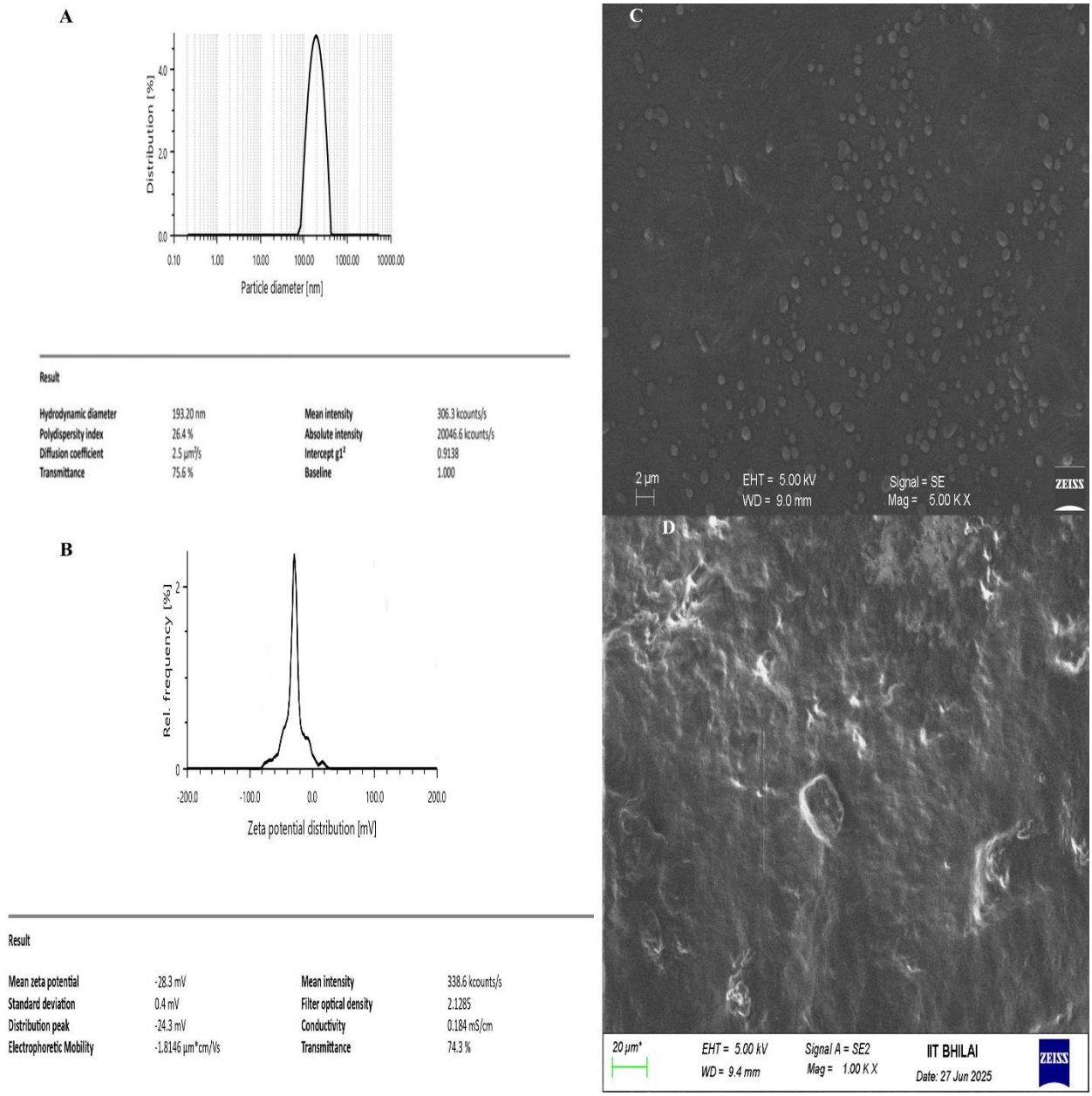

Figure 1. A. Particle size distribution report of Ibudilast-loaded Ethosomes B. Zeta potential graph of Ibudilast-loaded Ethosomes C. SEM image of the Ibudilast-loaded Ethosomes D. SEM image of Ibudilast-loaded Carbopol nanogel

Journal of Chemical Health Risks
www.jchr.org
JCHR (2025) 15(6), 571-584 | ISSN:2251-6727

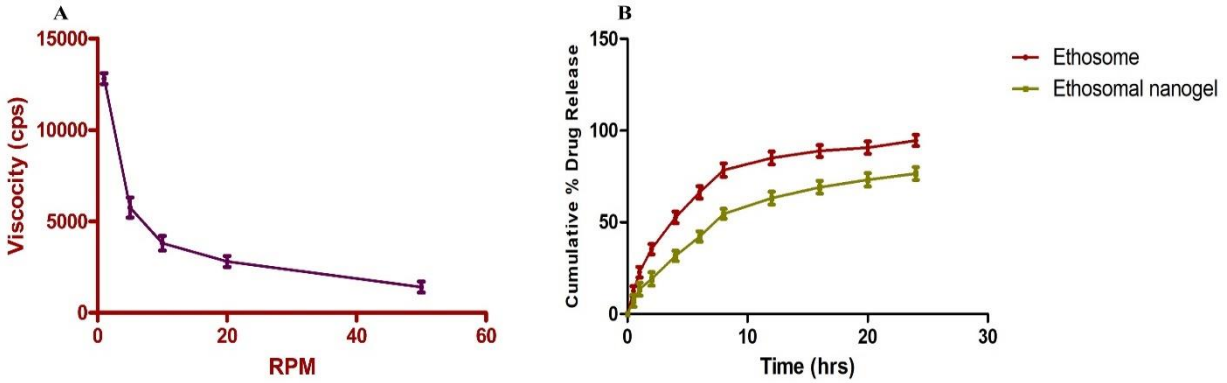

Figure 2. A. Effect of shear rate on the viscosity of ethosome-loaded Carbopol nanogel B. In vitro drug release study for Ibudilast-loaded Ethosomes and Ibudilast-loaded nanogel.

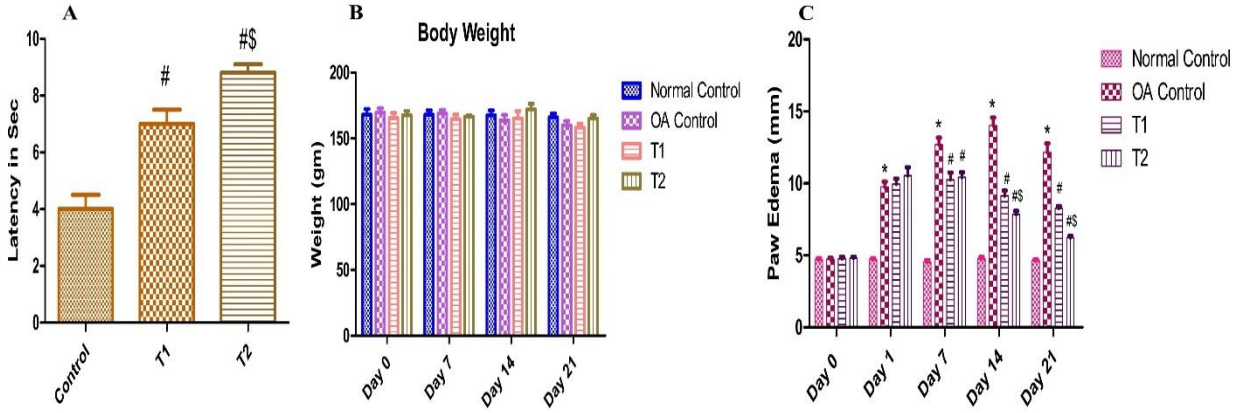

Figure 3. A. Effect of Ibudilast Regimens on analgesic activity in MIA-induced Osteoarthritis Rat B. Effect of Ibudilast Regimens on Body Weight Changes in MIA-induced Osteoarthritis Rat C. Effect of Ibudilast Regimens on paw volume changes in MIA-induced Osteoarthritis Rat

Values are represented as mean ±SD. Data were analyzed using two-way ANOVA followed by a Bonferroni post hoc test. *P<0.05 when compared to the normal group, #P<0.05 when compare to the OA control group and #$P<0.05 when compared to the T1 group.

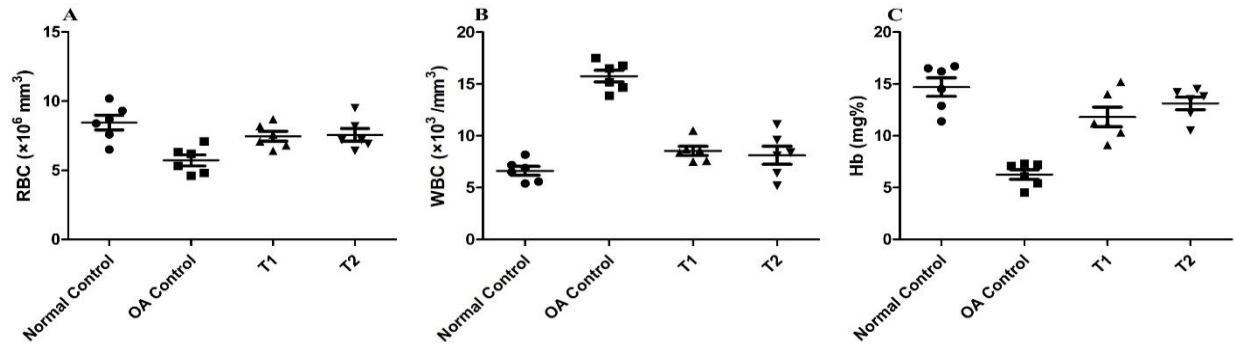

Figure 4: Effect of Ibudilast Regimens on Hematological Parameters in MIA-induced Osteoarthritis Rat

Values are represented as mean ±SD. Data were analyzed by using one-way ANOVA followed by Tukey post hoc test. *P<0.05 when compare to the normal group and #P<0.05 when compare to the OA control group.

Journal of Chemical Health Risks
www.jchr.org
JCHR (2025) 15(6), 571-584 | ISSN:2251-6727

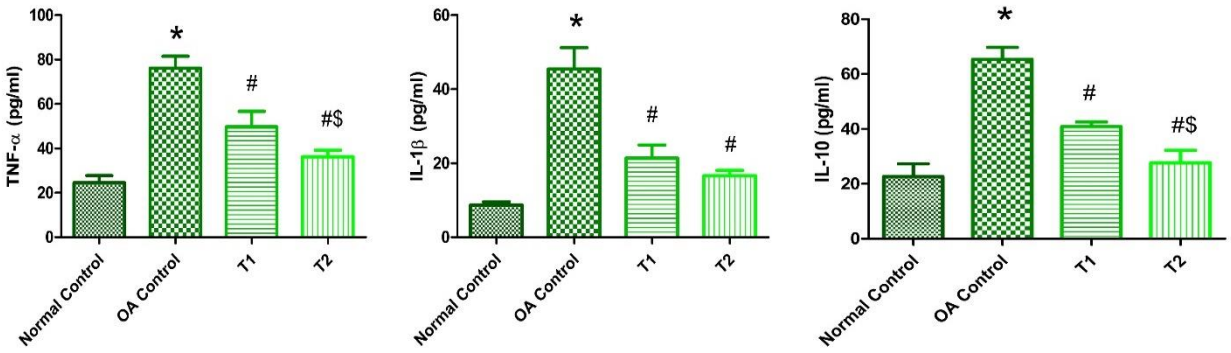

Figure 5. Effect of Ibudilast Regimens on Biochemical Parameters in MIA-induced Osteoarthritis Rat

Values are represented as mean ±SD. Data were analyzed by using one-way ANOVA followed by Tukey posthoc test. *P<0.05 when compare to the normal group, #P<0.05 when compare to the OA control group and #$P<0.05 when compared to the T1 group.

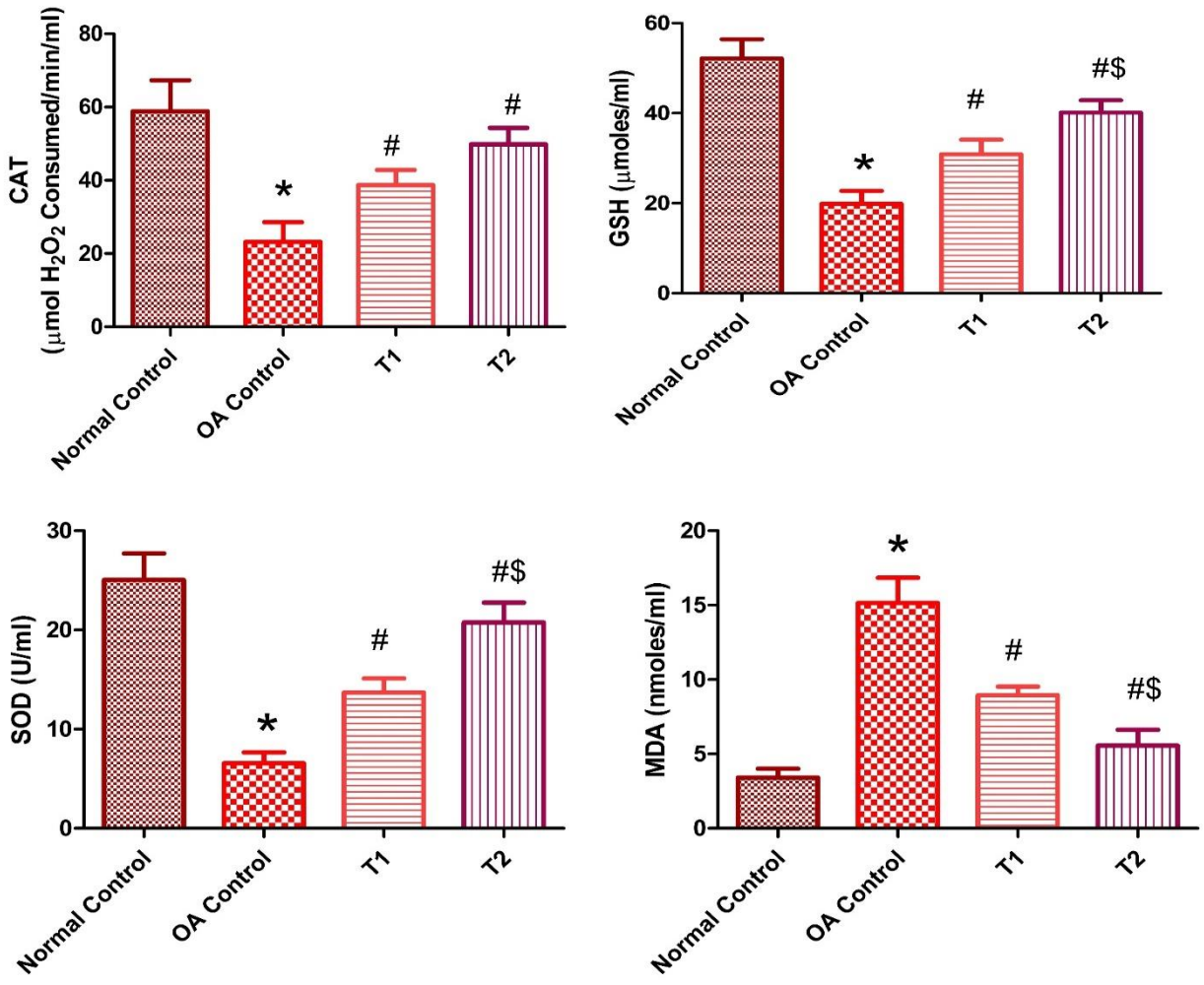

Figure 6. Effect of Ibudilast Regimens on Oxidative Parameters in MIA-induced Osteoarthritis Rat

Journal of Chemical Health Risks

www.jchr.org

JCHR (2025) 15(6), 571-584 | ISSN:2251-6727

Values are represented as mean ±SD. Data were analyzed by using one-way ANOVA followed by Tukey posthoc test. *P<0.05 when compare to the normal group and #P<0.05 when compare to the OA control group.

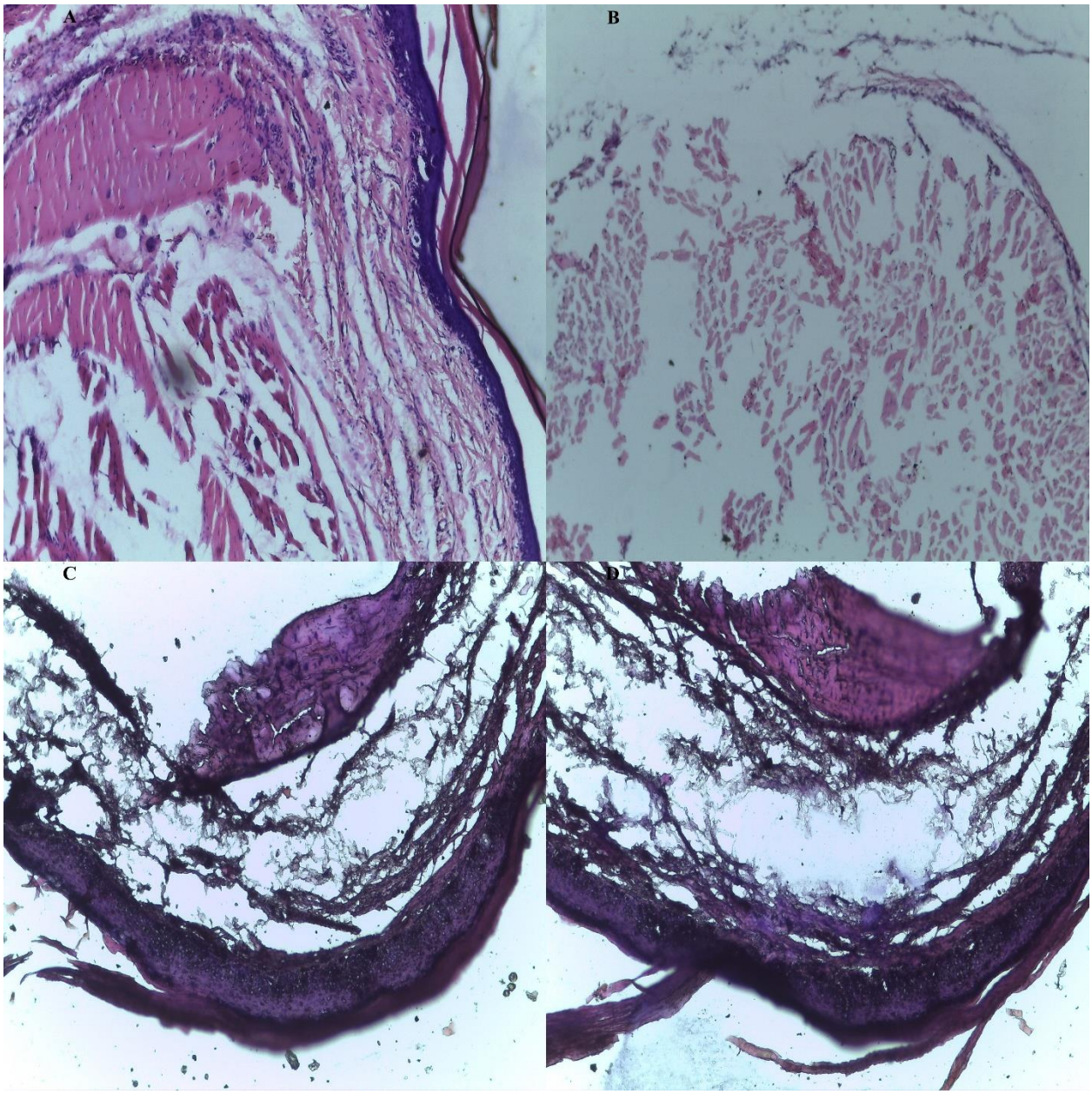

Figure 7. Histopathological Study Results (A) Normal control (B) OA Group (C) Plain ibudilast gel (D) Ibudilast-loaded Nanogel